

CHAPTER-4

Characterization and LCW mineralization potential of vermitechnology using selected earthworm species (*Eisenia fetida*)

4.1 Introduction

Nearly 50% of the solid waste generated in the world is biogenic and contains lignocellulosic substances [1]. According to a recent report, the annual global generation of lignocellulosic biomass is more than 200 billion tons, with paddy straw and food waste as the dominant components [2]. It has been estimated that more than 700 million tons of paddy straw are wasted annually worldwide [3]. Similarly, approximately 1052 million tons of foods were reported to be wasted in 2022, for an average per capita generation of 132 kg [4]. Apart from food scarcity and economic problems, food waste contributes approximately 8-10% of global greenhouse gas emissions, including from both loss and waste [4]. Paddy straw is chiefly composed of cellulose, hemicelluloses, and lignin, with the proportion of cellulosic substances being the highest [5]. The food waste generated worldwide has a similar predominance of lignocellulosic substances [6], which are integral components of plant cell walls, complex in structure, and inherently hydrophobic [7]. Complex networks of these polymeric compounds not only resist microbial intervention but also deactivate some vital enzymes [8]. The recalcitrance of lignocellulosic materials thus limits their efficient utilization, and appropriate treatment is required to successfully recover nutrients from these substances [9].

Composting and vermicomposting are key technologies for converting numerous types of solid waste into valuable organic fertilizers [10]. Composting technologies activate inherent microorganisms that can eventually drive the decay of organic substances. Vermicomposting takes advantage of synergy among earthworm activity, earthworm gut microorganisms, and microbial communities inherent in feedstocks [11,12]. Thus, both processes are tightly affected by the composition of the microbial communities driving decay.

The performance of vermicomposting systems is primarily governed by the nature and composition of feedstocks, earthworm compatibility, and microbial growth and activity

[13]. Lignocellulosic waste-based vermireactors often encounter high C/N ratios and crystalline polymeric structures that largely restrict microbial activity [14]. However, combining lignocellulosic biomass with readily decomposable substances such as municipal biosolids [15], cattle manure [16], or cow dung [14] can effectively facilitate earthworm–microbe interactions that can speed the mineralization of the biomass.

Previous 16S rRNA gene-based studies of bacterial and fungal communities provided only partial knowledge because numerous eukaryotic and prokaryotic organisms can arise during bio-composting [17,18]. A next-generation sequencing (NGS)-based whole metagenomic approach can properly and comprehensively assess the organismal diversity and functionality found in vermicomposting systems. Overall, the literature review identified the following research gaps. First, the Illumina NGS technique has not yet been used to assess the microbial diversity of a lignocellulosic (paddy straw and wasted food)-based vermicomposting system. Second, the influence of earthworms on the taxonomic and functional diversity of microbial communities during vermicomposting has yet to be compared with the conditions during aerobic composting. Third, little effort has been made to isolate beneficial microbial species from Illumina NGS-derived whole metagenomic information and thereby target specific vermicomposting feedstock.

Considering those research gaps, the present study was designed to investigate variations in microbial diversity during aerobic composting and vermicomposting of lignocellulosic waste (LCW, paddy straw and food waste) and identify how earthworms (*Eisenia fetida*) regulate microbial community structures in the end product. Temporal changes in various physicochemical and microbial attributes were assessed for two months. Eventually, one of the most enriched feedstocks from each condition (composting and vermicomposting) was selected for whole metagenome analyses on the Illumina NGS platform. To date, metagenomic approaches have been used to amass vast knowledge about microbial diversity in different environmental compartments. However, the practical utility of those big data has been explored rather scantily.

4.2 Materials and methods

Two experiments were conducted for assessing the microbial diversity in different types of lignocellulosic waste:

Table 4.1: Details of feedstock preparation and treatment names

Order	Vermicomposting with <i>E. fetida</i>		Aerobic composting	
1	CDv - Cow dung (CD)	V1	CDc - Cow dung (CD)	C1
2	PS+FW+CD(2:2:1)v: 2:2:1 mixture of paddy straw (PS), food waste (FW), & CD	V2	PS+FW+CD(2:2:1)c: 2:2:1 mixture of paddy straw (PS), food waste (FW), & CD	C2
3	PS+FW+CD(3:3:2)v: 3:3:2 mixture of PS, FW, & CD	V3	PS+FW+CD(3:3:2)c: 3:3:2 mixture of PS, FW, & CD	C3
4	PS+FW(1:1)v: 1:1 mixture of PS & FW	V4	PS+FW(1:1)c: 1:1 mixture of PS & FW	C4

4.2.1. Experiment-1: Bio-composting experiment and sampling

Food waste (FW) samples were collected from the waste disposal yard of Tezpur University, Assam, India, hostel kitchen (26.7008°N, 92.8303°E) in April 2022. At the same time, paddy straw (PS) and cow dung (CD) samples were collected from the agricultural field of a local farmer in Tezpur. The FW and PS samples were chopped into pieces of about 1×1 cm and spread under a shed in the vermiculture unit of the Department of Environmental Science at Tezpur University for seven days of pre-composting. The FW and PS biomasses were kept moist (~50-60% moisture content) by intermittent sprinkling of water. After precomposting all substrates were turned and stabilized at about 60±5% moisture content. Pre-composting is method of short period composting that helps to attain stable temperature within mesophilic range thereby accelerating the vermicomposting process [18,19]. The aerobic composting reactors and vermireactors were perforated truncated-cone-shaped earthen vessels (0.45m (width) × 0.45m (length) × 0.30m (width)) installed in the shaded portion of a yard. The vermibeds and composting beds (5 kg each) were prepared with various mixtures of FW, PS, and CD. Adult earthworms (*Eisenia fetida*) @ 10 worm kg⁻¹ were added to each vermicomposting feedstock. The use of adult (i.e., clitellated) earthworm specimens expedite the earthworm-mediated decomposition process and previous studies reported that a stocking density of 10 adult worm is sufficient to obtain high quality vermicompost [20,21]. Identical sets of treatment combinations (i.e., feedstocks) were placed in similar perforated truncated-cone-shaped earthen vessels for aerobic

composting, conducted without the presence of earthworms and under identical maintenance practices (e.g., watering and mixing). The composting and vermicomposting feedstocks were intermittently sprinkled with water to maintain optimum moisture content (50–60%), and they were regularly churned and turned to ensure adequate aeration. Daily records of moisture content were collected using a volumetric water content (VWC)-based soil moisture sensor, specifically the MODBUS- RTU RS485 (S-Soil MT-02A) model. This sensor reliably provides moisture content data in percentage with a high level of accuracy ($\pm 3\%$). Accordingly, water was sprinkled while simultaneously recording the moisture content using the VWC sensor. The experiment was conducted for two months (60 d) from May to June 2019. Watering was stopped on the 55th day, and on the 60th day, the earthworms were separated from the completed vermicompost by sieving and re-introduced to the vermiculture unit. Feedstock samples were drawn from all the feedstocks at 0, 30, 45, and 60 days for use in various analyses. The details of the different feedstocks are shown in Table 4.1.

4.2.2. Physicochemical and microbial assessments during composting and vermicomposting

The periodically collected vermicompost and compost samples were prepared for the analysis of various physical, chemical, and microbial attributes. In short, the feedstock samples were air dried in a dry platform under shed, chopped if needed, sieved (mesh size: BSS 30) to obtain homogeneous powdery particles, which were used for all physicochemical analyses. The physical variations in the samples were assessed based on bulk density (BD) [22,23], the x-ray diffraction (XRD)-derived crystallinity index (CI) [24], and scanning electron microscopy (SEM) [14]. The BD of the prepared feedstock samples was estimated with the help of pycnometer or specific gravity bottle. The feedstock samples (~100 mg) were subjected to glass sample holder of the X-ray diffractometer (Make/Model: Brucker D8) and analyzed in plateau conditions. The samples were fixed in dry acetone and embedded in PELCO flat embedding molds (Ted Pella, Redding, CA) followed by coating with dry ice in ethanol before capturing images in a scanning electron microscope (Make: JEOL; Model: JSM 6390LV).

The chemical attributes were analyzed by following standard methods (pH [23], electrical conductivity (EC) [22], total organic C (TOC) [25], total N (TN), available P [22], and available K [22]). For pH and EC estimation, samples were suspended in water (MilliQ) and 1:25 (w/v) and 1:5 (w/v) ratios, respectively and measurements were taken

in a digital pH meter and a conductivity meter, respectively. The TOC was estimated by potassium dichromate-sulfuric acid oxidation followed by heating till bubble appears and titration of the excess-dichromate with ferrous ammonium sulfate solution. The TN contents of samples was estimated by digesting the samples in presence of catalysts (sulfuric acid, copper sulfate, and potassium sulfate) at 420°C and subsequent distillation in a Kjletec digestion-distillation system (FOSS, Denmark) followed by collection of distillates in acid (0.1 N H₂SO₄) and titrating with alkali (0.1 n NaOH). For estimation available P concentrations, samples were extracted either with NaHCO₃ (Olsen extraction: for sample pH > 6.0) or with NH₄F (Bry's extraction: for sample pH < 6.0) and analyzed in an UV-Vis spectrophotometer using ammonium molybdate-based reagents (Cary 60, Agilent, USA). On the other hand, CH₃CO₃NH₄ extraction technique was followed estimation of the available K concentrations in a flame photometer (Systronics, India). Changes in microbial activity were evaluated based on microbial respiration (MR), microbial biomass C (MBC), and total bacterial and fungal counts. The phenolphthalein titration method for assessing microbe-respired carbon dioxide evolution was adopted to measure MR kinetics in the samples [26]. The chloroform fumigation-based assay was undertaken to evaluate MBC in the samples [27]. The total bacterial and fungal populations in the compost and vermicompost samples were enumerated after Parmer and Schmidt (1964) [28]. In short, the microbial colonies developed on specific media (nutrient agar for bacteria and potato dextrose agar for fungus) were counted by a colony counter to compute the number of colony-forming units ml⁻¹.

The methodologies adopted for the studied attributes are discussed in detail as below:

4.2.2.1. Physical properties [29]

A. Measurement of bulk density (BD)

Procedure:

The bulk density was determined by using the disturbed method. This method is used when it is not possible to take a consolidated sample, as in sandy soils and soils of greenhouses and nurseries, because they are loose and very friable. At the beginning the weight of the core sampler (W₁ g) was taken. It was then placed into the surface of the

sample and taken back. This was done to collect sample having same volume as that of the core sampler (V ml), the mouth of the sampler was cleaned. The sample inside the core sampler was taken out and dried at 105 °C in a hot air oven till a constant weight was obtained. After that, the oven dry sample was weighed along with the core sampler (W₂ g).

Calculation:

$$\text{Bulk density of sample, BD} = \frac{(W_2 - W_1)}{V} \text{ g cc}^{-1}$$

Where,

V: Volume of the core sampler bottle

B. Measurement of Crystallinity index (CI)

Procedure:

The homogeneous powdery feedstock samples (~100 mg) were subjected to glass sample holder of the X-ray diffractometer (Make/Model: Brucker D8) and analyzed in plateau conditions. Correspondingly, the CI was computed based on the intensity of crystalline plane (002) and amorphous plane using the below calculation.

Calculation:

$$\text{CI} = \frac{((I_{002} - I_{amor}))}{I_{002}} \times 100$$

Where,

CI = crystallinity index

I₀₀₂ (crystalline)= intensity at 22.8°

I_{amor}= intensity at 18°

4.2.2.2. Chemical properties [29]

A. Measurement of samples pH:

Procedure:

About 10 g of sample was weighed in a beaker and 25 ml distilled water was added to it to prepare a suspension of 1::2:5. The solution was stirred intermittently with a glass rod about 1 hour. The pH of the suspension was recorded with the help of EuTech pH meter.

B. Estimation of Total Organic Carbon (%)

1g of experimental sample was taken in a conical flask and to it 10 mL potassium dichromate and 20 mL of concentrated sulphuric acid was added. The samples were heated for a while till bubbles occurred. It was then kept some time for cooling and then 200 mL of distilled water was added. Afterwards, 1.5 mL of diphenylamine indicator was added following the addition of 10 mL of orthophosphoric acid. It was then titrated with ferrous ammonium sulphate solution till the occurrence of dark green colour.

Calculation:

$$\text{Total Organic carbon (\%)} = \frac{V_k \times \left(1 - \frac{v_s}{v_b}\right)}{W} \times S_k \times 0.3$$

Where,

V_k : Volume of $K_2Cr_2O_7$ Solution

V_s : Titrant reading

V_b : Blank reading

S_k : Strength of $K_2Cr_2O_7$ Solution

W : Weight of soil sample

For example,

Weight of the sample= 'W' g

Volume of $K_2Cr_2O_7$ solution= X mL

Titrant reading of the sample= A mL

Titrant reading of the sample= B mL

Strength of $K_2Cr_2O_7$ Solution = C

$$\text{Total organic carbon(\%)} = \frac{X \times (1 - \frac{A}{B})}{W} \times C \times 0.003 \times 100$$

Where, 0.003 = 1 ml of N Potassium dichromate will be equal to 0.003 gm carbon.

C. Determination of Total nitrogen (%)

The soil is digested in concentrated H_2SO_4 with a catalyst mixture to raise the boiling temperature and to promote the conversion from organic-N to NH_4^+ -N. The NH_4^+ -N from the digest is obtained by steam distillation, using excess NaOH to raise the pH. The distillate is collected in saturated H_3BO_3 , and then titrated with dilute H_2SO_4 to pH 5.0. The method determines ammonium-N, most of the organic-N forms, and a variable fraction of nitrate-N in soil

Procedure:

Take 1 g soil sample, add 0.8 g $CuSO_4$ and 7 g K_2SO_4 . Then add 12- 15 mL conc. H_2SO_4 . Digest the contents at $420^\circ C$ for 1 hr, keep it to cool and transfer the contents to distillation flask and add 80 mL distilled water followed by 50 ml 40% NaOH until the appearance of black colour. Then, start distillation and the distillate is collected in a conical flask containing 20 ml 0.1 N H_2SO_4 and 3-4 drops of mixed indicator. Finally titrated with 0.1 N NaOH.

Calculation:

Total Nitrogen (%) = (Volume of H_2SO_4 × strength – Volume of NaOH consumed × strength) × 0.014 × 100) ÷ Weight of soil

D. Estimation of Available P ($mg\ kg^{-1}$)

The estimation of available P was done by Olsen extraction method when pH of the sample was more than 6, whereas for pH less than 6 the concentration was measured following Bray-Kurt's method.

1. Estimation of available P by Olsen extraction method

Preparation of standard curve: 1, 2.5, 5.0, 7.5, 10.0, 12.5, 15.0 and 20.0 ml of 2 ppm standard P solution were pipetted in individual 50 mL Volumetric flasks. 3 drops of

dinitrophenol were added to each flask. To each solution, drop wise 4N NH_4OH was added till yellow color appears. Then 4 N HCl was added drop by drop until yellow color disappears and thus, pH of each solution was adjusted to 3. To each flask, 10 mL of $(\text{NH}_4)_6\text{Mo}_7\text{O}_{24} \cdot 4\text{H}_2\text{O}$ solution and 2,3 drops of SnCl_2 solution was added. The volume was made up to the mark and the reading was recorded against blank solution at 660 nm in UV-Visible spectrophotometer. Optical density reading was then plotted against standard concentration and a curve was drawn (Annexure A).

Procedure:

2.5 g sample was weighed in a 250 mL conical flask and 50 mL of extractant [0.5M NaHCO_3 (pH 8.5)] solution was added. The flasks were loaded on a mechanical shaker and vigorously shaken for 30 minutes. After 30 minutes, the soil emulsion was filtered through Whatman (no.42) filter paper. If yellow colored aliquot was observed then a spoon of P-free charcoal was added and filtered again. 5 ml of filtrate was transferred to a 50 mL Volumetric flask and 4 to 5 drops of dinitrophenol 4N NH_4OH and 4N HCl were added sequentially. Subsequently, 5 mL of ammonium molybdate was added to each flask followed by 2-3 drops of (5%) stannous chloride and then, volume was made up to 50 mL with distilled water. The solution was then mixed well and its absorbance was read at 660 nm.

Calculation:

$$\text{Available P (mg kg}^{-1}\text{)} = \text{Absorbance} \times \text{Slope} \times \text{dilution factor}$$

II. Estimation of available P by Bray-Kurt's method

Procedure:

2.5 g sample was weighed in a 250 mL conical flask and 25 ml of extractant 0.03 N NH_4F solution was added. The flasks were loaded on a mechanical shaker and vigorously shaken for 30 minutes. After 30 minutes, the soil emulsion was filtered through Whatman (no.42) filter paper. If yellow colored aliquot was observed then a spoon of P-free charcoal was added and filtered again. 5 mL of filtrate was transferred to a 50 mL volumetric flask and 4 to 5 drops of dinitrophenol, 4N NH_4OH and 4 N HCl were added sequentially. Subsequently, 5 mL of ammonium molybdate was added to each flask followed by 2-3 drops of (5%) stannous chloride and then, volume was made

up to 50 mL with distilled water. The solution was then mixed well and its absorbance was read at 660 nm.

Calculation:

$$\text{Available P (mg kg}^{-1}\text{)} = \text{Absorbance} \times \text{Slope} \times \text{dilution factor}$$

Estimation of exchangeable K

$$\text{Available K (mg kg}^{-1}\text{)} = \text{K concentration} \times \text{dilution factor}$$

For example,

Weight of the sample = 'W' g

Volume of extractant = 'A' mL

Dilution factor = B/W

Reading of flame photometer = 'X'

ppm K obtained from standard curve corresponding to X= R

$$\text{Available K (mg kg}^{-1}\text{)} = R \times B/W$$

E. Estimation of Available potassium (mg kg⁻¹)

This fraction of soil K is the sum of water-soluble and exchangeable K. The method uses a neutral ammonium acetate solution (1 N) to replace the cations present on the soil exchange complex. This is considered as plant available K in the soils, and is commonly measured by the flame photometer. However, the cation concentrations determined by this method are referred to as “exchangeable” for non-calcareous soils. For calcareous soils, the cations are referred to as “exchangeable plus soluble”.

Procedure:

1. Take 2g of sample in a 250ml conical flask.
2. Add 20 ml of 1N CH₃COONH₄ to it and shake for 30 minutes on a mechanical shaker.

3. Now filter the content and measure the available K in the filtrate by flame photometer

Calculation:

Total K= K concentration \times 10(dilution factor)

F. Urease activity ($\mu\text{g g}^{-1} \text{h}^{-1}$)

Calibration curve: 0, 0.5, 1, 1.5 and 2.0 $\mu\text{g mL}^{-1}$ $\text{NH}_4\text{-N}$ standards were taken in 5 different volumetric flasks. Then, 750 μL of urea solution was added and incubated at 37°C for 2 hrs and subsequently, the incubated solution was centrifuged (3000 rpm) for 2 minutes. 2.5 mL of NaOH-Na salicylate mixture solution was added along with 1 mL Na iso cyanurate solution. Afterwards, the optical density was recorded in 690 nm (see Annexure A).

Calculation:

$$\text{Urease activity } (\mu\text{g g}^{-1} \text{h}^{-1}) = \frac{\text{OD Sample} - \text{OD Blank}}{\text{Slope} \times T \times W}$$

Where,

OD = Optical density

T = Time for incubation

W = Weight of the sample

G. Phosphatase activity ($\mu\text{g g}^{-1} \text{h}^{-1}$)

Calibration curve: 1 mL of standard p-nitrophenol solution was diluted to 100 mL in a volumetric flask. Then, 0, 1, 2, 3, 4 and 5 mL aliquot of this standard solution was pipetted in 50 mL Erlenmeyer flasks. The volume was adjusted to 5 mL by addition of distilled water. Then, 5 mL of 0.5 M CaCl_2 solution, 1 mL of PNPP Solution were added in to each flask. The contents were shaken vigorously and filtered. Absorbance was measured at 400 nm. (See Annexure A).

Procedure:

2g of soil sample was taken in a test tube and 5 mL of 0.5 M CaCl₂ solution was added and mixed vigorously. 1 mL of PNPP solution was pipetted into each test tubes. 1 mL of phosphate buffer was added to the tubes and incubated at 37°C for 1 h. The contents were centrifuged at 4000 r = rpm for 5 minutes. 3 mL of this clear supernatant was transferred to clean test tubes. A sample blank was prepared similarly taking only phosphate buffer in place of sample. Absorbance was recorded at 440 nm in a spectrophotometer.

Calculation:

$$\text{Phosphatase activity } (\mu\text{g g}^{-1} \text{ h}^{-1}) = \frac{OD \text{ Sample} - OD \text{ Blank}}{\text{Slope} \times T \times W}$$

Where,

OD = Optical density

T = Time for incubation

W = Weight of the sample

H. Compost respiration

Principle: Microbial respiration in sample is a measure of cumulative respiration of both the aerobic and anaerobic microbe present in the sample, that evolves due to microbial metabolism during the decomposition of organic matter present in the sample, Microbial respiration is measured by evaluation of CO₂ due to microbial metabolism. CO₂ evolved is absorbed in NaOH or KOH solution and then the solution is titrated with HCl in presence of phenolphthalein indicator.

Procedure:

10 g of moist soil sample was taken in a 500 mL corked conical flask. In a 10 mL test tube, 1 ml of distilled water and 5 mL of 0.1 N NaOH was taken and placed inside the flask. The mouth of the conical flask was corked and incubated at 25°C for 24 hours. After 24 hours, the test tubes were taken out from the flask and the solution was transferred to a 100 mL conical flask with the addition of 5 mL distilled water. Then 5 mL of BaCl₂ was added in the solution followed by 3 drops of phenolphthalein indicator.

The solution was titrated with 0.05 N HCl till it turned colourless from pink and the burette reading was noted.

Calculation:

$$\text{Compost respiration } (\mu\text{g g}^{-1} \text{ h}^{-1}) = \frac{(V_0 - V_t) \times 100 \times \delta}{(M_w - M_d) \times t}$$

V_0 = Blank titrated value

V_t = Sample titrated value

δ = Strength of HCl

M_w = Weight of the moist soil

M_d = Weight of the oven dry soil

t = Time of incubation

I. Obstinate C fractions (humic acid C and fulvic acid C)

Procedure:

5g sample was extracted in 100 mL of sodium pyrophosphate solution, shaken for 30 minutes and kept overnight. Next day the solution was filtered. 5 mL of the filtrate was taken and analyzed for total organic C following modified Walkley and Black. The remaining filtrate was acidified with 10 mL of concentrated H_2SO_4 (pH at 2-3) and kept overnight. This is done because the addition of concentrated acid precipitates the humic substances. The resultant precipitate was filtered and FAC was enumerated by taking 5 mL of the filtrate as mentioned for the estimation of TOC. The precipitate adhered on the surface of the filter paper was washed with 20 mL of 0.1 N NaOH and 5 ml of this suspension was used for determining the HAC content as mentioned in page no...

Calculation:

$$\text{Total organic C (\%)} = \frac{Vk \times (1 - vs/vb)}{W} \times Sk \times 0.3$$

$$\text{Fulvic acid C (\%)} = \frac{Vk \times (1 - vs/vb)}{W} \times Sk \times 0.3$$

$$\text{Humic acid C (\%)} = \frac{Vk \times (1 - vs/vb)}{W} \times Sk \times 0.3$$

Where,

V_k : Volume of $K_2Cr_2O_7$ solution

V_s : Titrant reading

V_b : Blank reading

S_k : Strength of $K_2Cr_2O_7$ solution

W : Weight of soil sample

For example,

Weight of the sample= 'W' g

Volume of $K_2Cr_2O_7$ solution = X mL

Titrant reading of the sample= A mL

Titrant reading of the blank= B mL

Strength of $K_2Cr_2O_7$ solution = C

$$\text{Total organic carbon (\%)} = \frac{X \times (1 - A/B)}{W} \times C \times 0.003 \times 100$$

Where, 0.003 = 1 mL of N Potassium dichromate will be equal to 0.003 g carbon.

4.2.3. SEM

Scanning electron microscope (SEM) (Make: JEOL, JSM-6390 Japan) derived images were obtained to study the physical microstructural composition of LCW samples. The samples were fixed in dry acetone and embedded in PELCO flat embedding molds (Ted Pella, Redding, CA) followed by coating with dry ice in ethanol before capturing images in a scanning electron microscope (Make: JEOL; Model: JSM 6390LV). Sample preparation was done following the standard protocol [30], and image was taken at 300-500 X.

4.2.4. Microbial analyses

To quantify the bacterial load, 1 g of air-dried samples dried sample was mixed with 10 ml of deionized water and allowed to vortex for 15 minutes. The samples were then serially diluted from 10^{-1} to 10^{-6} respectively. Desired amount of aliquot (0.1 mL) was suspended in the petriplates containing nutrient agar (NA) (for total count), Pikovskaya agar (PA) (for P-solubilizing colonies), and Burk's medium (B) (for N-fixing colonies) [11]. This work was performed in the laminar air flow chamber to prevent external contamination. Then, the inoculated petriplates were kept in incubators for microbial proliferation (NA plates for total bacterial count were incubated at 37°C for 24 h; PA and B plates for P-solubilizing and N-fixing microbial count were incubated at 28 °C for 48h). The colonies grown in the petriplates after incubation were counted with the help of colony counter and the colony forming unit (CFU) was calculated by the formula given below [11].

$$\text{No. of organism } m L^{-1} = \frac{\text{No. of colonies} \times \text{dilution}}{\text{Amount plated}}$$

The isolated NFB and PSB colonies were repeatedly streaked on Burk's and Pikovskaya agar medium respectively to obtain pure cultures.

4.2.5. Next generation sequencing and metagenomic analysis

The feedstocks most optimally degraded by vermicomposting and composting, according to the results of the physicochemical and microbial analyses during the bio-composting experiment, were selected for detailed microbial community assessment via NGS. The Illumina platform was used to efficiently characterize the metagenomic diversity of both culturable and non-culturable microbial groups. The DNA in all the given samples was isolated with an Xcel Gen soil DNA isolation kit (Xcelris Labs Limited, Gujarat, India). The DNA quality was verified on a 0.8% agarose gel to ensure the achievement of a single intact band on gel electrophoresis (110 V for 30 min).

A satisfactory amount of DNA (200 ng) was used to initiate the library preparation process. The DNA samples were mechanically split into smaller fractions, and the end-repair step was conducted continuously. Subsequently, platform-specific adapters were tied to both ends of the DNA fragments. The adapters are loaded with essential

sequences to promote the binding of dual bar-coded libraries to a flow cell for sequencing. This facilitated both polymerase chain reaction (PCR) amplification of the tied-up DNA fragments and binding with the standard Illumina sequencing primers. Moreover, a high-fidelity amplification step was performed in a HiFi PCR master mix to maximize the yield of microbial DNA. The quality of the amplified library was assessed in a Bioanalyzer 2100 (Agilent Technologies) using a high-sensitivity DNA chip. Afterward, the libraries were loaded onto the Illumina platform for cluster generation and sequencing [31]. The next generation sequencing for all the samples was performed in Illumina Platform with a chemistry of 2×150 basepair (bp).

4.2.5.1. Metagenome assembly

De novo assembly of high quality paired-end (PE) reads was accomplished using CLC genomic Workbench 6.0 software at default parameters (minimum contig length: 200; automatic word size: Yes; perform scaffolding: Yes; Mismatch cost: 2, Insertion cost: 3, Deletion cost: 3, Length fraction: 0.5, Similarity fraction: 0.8). The statistical elements of the assemblies were calculated by in-house scripts and the results are given in Table 4.2. The gene prediction of the assembled scaffolds for all samples was performed using Prodigal (v2.6.3). Statistics for genes prediction are provided in Table 4.3.

Table 4.2: Statistical elements of the assemblies of two different treatment combination.

Assembly	Scaffolds	Total Scaffold length(bp)	Average Scaffold length(bp)	Scaffold N50 (bp)	Max Scaffold size(bp)
LCWv	85346	89220879	1045.4	1423	122139
LCWc	81835	87644849	1070.9	1274	50791

Table 4.3: Statistics for genes prediction in two different treatment combination.

Treatments	No. of genes	Total genes size (bp)	Average genes size (bp)	Max gene size (bp)
LCWv	84348	51583905	611	16725
LCWc	88324	50712813	574	9435

4.2.5.2. Taxonomic and functional annotation

Taxonomic metagenomic annotation was conducted using Kaiju. Kaiju is a fast, free, sensitive, and standalone metagenome classifier which finds maximum exact matches on the protein-level using the Burrows Wheeler transform algorithm [32]. Kaiju classifies individual metagenomic reads using a reference database comprising the annotated protein-coding genes of a set of microbial genomes. By default, Kaiju uses either the available complete genomes from NCBI Ref Seq or the microbial subset of the non-redundant protein database nr used by NCBI BLAST, optionally also including fungi and microbial eukaryotes. Kaiju translates metagenomic sequencing reads into the six possible reading frames and searches for maximum exact matches (MEMs) of amino acid sequences in each database of annotated proteins from microbial reference genomes and optionally perform searches using GREEDY algorithm. In this study, the GREEDY run mode was used with a minimum match length of 11, minimum match score of 75, and 5 permitted mismatches. The functional capacity of the microbial communities was evaluated using COGNIZER (v0.9b) at default parameters. COGNIZER is a comprehensive stand-alone framework, enabled to simultaneously provide COG, KEGG, P fam, GO, and FIG fams annotations to individual sequences constituting metagenomic datasets.

4.2.6. Experiment-2: Vermicomposting and composting with lignocellulosic biomass

Vermicomposting was conducted with lignocellulosic waste (vegetable peels, sugarcane bagasse, and rice straw) materials to stimulate cellulose-degrading and ethanologenic microorganisms. The lignocellulosic waste materials were homogenized with urine-free cow dung at a ratio of 3:1. The vermibeds and composting beds were prepared in truncated cone-shaped earthen reactors of 3L capacity [0.45m (height)×0.15m (base radius)×0.30m (top radius)]. The feedstocks were pre-composted for five days prior introduction of earthworms in the vermireactors for the thermo-stabilization [33]. Eventually, non-clitellated juvenile *E. fetida* specimens (10 earthworm kg⁻¹) were employed in the vermireactors. The incubation was carried out for 60 days by maintaining 40-50% moisture within a temperature range of 27-30°C, and aeration was maintained by intermittent mixing of the feedstocks throughout the incubation period. The whole set of vermicomposting and composting reactors was replicated thrice. Feedstock samples were periodically drawn at 0, 30, and 60 days to assess the physicochemical and microbial changes during biomass degradation.

4.2.7. Analysis of physicochemical and microbial properties in feedstocks

The periodically obtained vermicompost and compost samples were analyzed for pH, total N, available P, and exchangeable K by following standard protocols [22]. The microbial activity in the compost and vermicompost feedstocks was assessed based on microbial respiration and microbial biomass C (MBC). Microbial respiration was measured by estimating the CO₂ emitted from the samples on incubation with glucose in a closed system at 25°C for 24 hours. The MBC was estimated by the fumigation extraction technique as detailed by Jenkinson (1988) [27]. In short, compost and vermicompost samples were fumigated in the presence of chloroform. After that, fumigated and un-fumigated samples were extracted in 2M KCl, and the ninhydrin-N level in the filtrates was spectrophotometrically assessed at 570 nm. All analyses were performed in clean glassware rinsed with deionized water. Analytical grade reagents and deionized water were used for preparing all the solutions [34]. In addition, the total bacterial and fungal counts in the compost and vermicompost samples were analyzed by pour plate technique using nutrient agar (NA) and potato dextrose agar (PDA), respectively [11]. The colony forming units (CFU) mL⁻¹ were calculated with the help of the formula given below:

$$\text{No. of organism } m L^{-1} = \frac{\text{No. of colonies} \times \text{dilution}}{\text{Volume plated}}$$

4.2.8. Waste to wealth conversion efficiency and economic evaluation

Waste-to-wealth conversion efficiency (WCE) of vermicomposting and aerobic composting systems was computed by modifying the formula given by Lalander et al. (2015) [35] to ascertain their environmental compatibility, as shown below.

$$\text{Waste conversion efficiency (WCE)} = \frac{\text{Nutrient} - \text{Enriched end product fresh weight (kg)}}{\text{Initial feedstock fresh weight (kg)}} \times 100$$

Moreover, the economic feasibility of both systems was evaluated on a large-scale basis (100 kg capacity) followed by computing the benefit-cost ratio (BCR) according to the formula given by Dilon and Hardaker, 1993 [36].

$$\text{Benefit cost ratio (BCR)} = \frac{\text{Gross return (Rupees)}}{\text{Total operational cost (Rupees)}}$$

Where,

Gross return

= *Present market price of the end product (i. e., vermicompost or Compost)*

× *Total quantity produced (kg)*

The details of the variables considered for the above calculations are provided in the below Table 4.4

Table 4.4: Variable/Item details for computation of waste recovery efficiency (WCE) and benefit-cost ratio (BCR) for vermicompost and compost.

For Vermicompost	
Particulars	Variable Cost (Rs./kg) for 100 kg total biomass
Cow dung price	5
Lignocellulosic waste collection	5
Earthworm price	50
Transportation cost	440
Labor charges	2500
Total Variable Cost (Rs/kg)	3000

For Compost	
Particulars	Variable Cost (Rs/kg) for 100 kg total biomass
Cowdung	5
Lignocellulose	5
Transport	440
Labours	2500
Total Variable Cost (Rs/kg)	2950

4.2.9. Statistical analyses

The temporal data from the bio-composting experiment were analyzed in SPSS using two-way ANOVA followed by the least significant difference (LSD) test to differentiate the efficiency of the various treatments at a significance level of $p < 0.05$.

4.3. Results and Discussion

Two experiments are detailed in the materials and method section (Section no. 4.2) have been conducted for evaluating the dynamics of microbial activities and their interaction with the changes in physico-chemical properties of the feedstocks in presence and absence of earthworms. Hence, the dynamics of physico-chemical and microbial attributes pertaining to each experiment have been discussed separately.

4.3.1. Chemical and microbial changes of composting and vermicomposting beds – determining the source viability for potential ethanol producers

Composting and vermicomposting were primarily conducted to create a microbe- enriched substrate, which could be used as a ready source for ethanol-producing microorganisms. The changes in the chemical and microbial properties of the vermibeds and composting beds are presented in Table 4.5. The pH sharply reduced under composting and vermicomposting, strongly indicating the microbe-induced organic matter decomposition process [19]. However, the increment in NPK bioavailability was significantly greater under vermicompost than under composting. This suggests that the presence of earthworms augmented the nutrient levels by accelerating the microbial activity [37]. Correspondingly, the microbial biomass carbon and microbial respiration were remarkably enhanced by about 3.35 folds and 2.31 folds in the vermibeds compared to the composting beds (P for treatment < 0.01 ; $LSD = 15.94$). These results indicate that microbial proliferation and activity were considerably more remarkable in the vermibeds than in composting beds. The results of the total bacterial and fungal count (Table 4.5) also strongly substantiated that microbial growth was significantly promoted under vermicomposting. Earthworms enrich the microbial diversity in vermibeds by contributing through their intestinal microflora [11]. Hence, we postulated that the vermibeds would be better substrates for searching for potential ethanol-producing organisms than the composting beds.

Table 4.5: Temporal changes in pH, available P (Av P), total Nitrogen (TN), exchangeable K (Av K), Compost respiration (Comp. Res), Microbial biomass carbon (MBC), bacterial and fungal count during the bioconversion experiment (mean±standard deviation)

Parameters	Compost			Vermicompost			P values			
	0D	30D	60D	0D	30D	60D	P _{treatment}	P _{time}	P _{treatment×time}	LSD _{treatment}
pH	8.49±0.18	8.38±0.29	6.44±0.34	8.15±0.12	8.33±0.18	6.36±0.25	NS	<0.01	NS	-
Av P (mg kg ⁻¹)	26.41±0.28	40.22±0.18	63.34±0.42	27.56±0.4	51.42±0.36	78.37±0.26	<0.01	<0.01	<0.01	10.65
Total N(%)	0.34±0.12	0.61±0.1	0.64±0.12	0.55±0.12	0.70±0.14	0.85±0.10	NS	<0.01	NS	0.06
Av K (mg kg ⁻¹)	34.33±0.20	54.48±2.87	62.45±0.38	32.47±0.40	60.53±0.27	76.38±0.2	<0.01	<0.01	<0.01	8.69
Comp. Res (mg kg ⁻¹)	5.29±0.35	7.53±0.35	10.44±0.43	7.42±0.2	10.4±0.36	17.32±0.29	<0.01	<0.01	<0.01	7.84
MBC (mg kg ⁻¹)	85.60±0.44	185.30±3.3	215.94±6.81	85.8±14.04	248±34.3	259.08±37.25	<0.01	<0.01	<0.01	15.91
Bacterial count [log(CFU)]	7.06±0.03	-	7.64±0.005	8.16±0.02	-	8.21±0.02	<0.01	<0.01	<0.01	-
Fungal count[log(CFU)]	6.03±0.08	-	6.2±0.08	6.5±0.02	-	6.94±0.01	<0.01	<0.01	<0.01	-

4.3.2. Physical changes in feedstocks under composting and vermicomposting

The effects of earthworms and microbial activity on the physical characteristics of the feedstocks were studied based on temporal changes in BD, CI, and a SEM-based structural analysis. In general, the BD decreased sharply in all feedstocks, and the rate of BD reduction was significantly high in V4 and V1 (Fig. 4.1a; $P < 0.01$; $LSD = 0.019$).

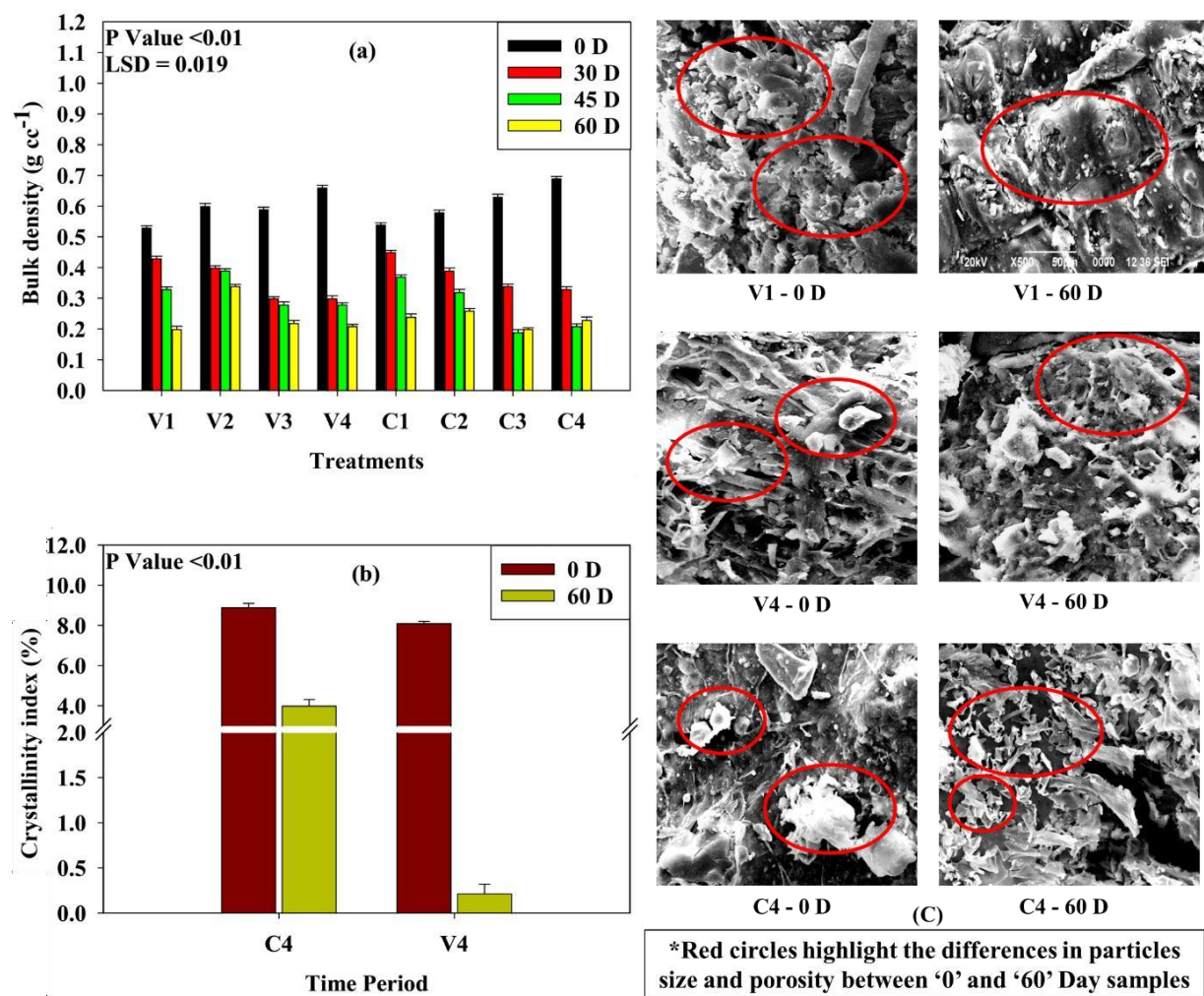


Figure 4.1: Changes in the physical properties of lignocellulosic feedstocks during composting and vermicomposting. a. Bulk density. Values represent the mean±standard deviation (n=3); b. Crystallinity index. Values represent the mean±standard deviation (n=3); and c. Scanning electron microscopy-based structural analysis of different feedstocks during incubation.

Earthworms are prolific grinders because of their efficient gizzards [38]. Such a significant reduction in the BD of the PS+FW(1:1)v feedstock under vermicomposting

might have been due to breakdown of the crystalline framework of the lignocellulosic substances. The crystallinity of lignocellulosic materials has been reported to greatly resist microbial-induced decomposition [24]. To assess the functional role of the earthworm-mediated biomass decomposition process, the XRD-based CI for the feedstocks was calculated (Fig. 4.1b). Interestingly, the CI value of V4 exhibited a nearly nine-fold decrease relative to that in the C4 sample. The temporal decline in CI implies the breakdown of the crystalline framework of the biomass [24]. Moreover, differences in the SEM images of V4 and C4 further confirm that the earthworms facilitated the microbial decay of the LCW-feedstocks (Fig. 4.1c). The SEM images show that crystallinity was initially high in both treatments, and after 60 days, it had a clear appearance of porous structures. The porosity was more prominent in the vermicompost than the compost.

4.3.3. Changes in the chemical characteristics of different lignocellulosic feedstocks

The data on changes in EC, pH, TOC, TN, and available P and K are presented in Fig 4.2. EC, pH, and TOC decreased over time under composting and vermicomposting, however, the extent of reduction was significantly greater in the vermibeds than in the composting beds (14–46%) ($P_{\text{treatment}} < 0.01$; Fig. 4.2a–c). The EC steadily reduced in all treatments, and it was lowest in V2 followed by V3 and V4 vermibeds at 60 d (LSD = 0.013; Fig. 4.2a). In contrast, a rapid decline in pH (9–24%) towards acidic range was recorded during the first 45 days of vermicomposting and composting with subsequent rise in the pH toward neutrality in LCW-based feedstocks (Fig. 4.2b). Interestingly, the pH increment after 45 d was more significant in V2 (~45%) and V3 (~34%) than the other treatments (LSD = 0.09). In contrast, reduction in EC and TOC was constant and significant throughout the whole period of the study in all treatments (Fig. 4.2c). In the end, the lowest TOC was recorded in V3 [(PS+FW+CD(3:3:2)v)] followed by V2 [(PS+FW+CD(2:2:1)v)], V4 [PS+FW(1:1)v], and V1 (CDv) vermibeds ($P_{\text{treatment}} < 0.01$; LSD = 0.19). Eventually, more remarkable increase in TN was evident in the vermibeds than the composting beds (Fig. 4.2d). The final TN level in different feedstocks was in the order: V3 = V4 \geq V1 > C1 > V2 = C4 > C3 ($P < 0.01$; LSD = 0.03; Fig. 4.2d).

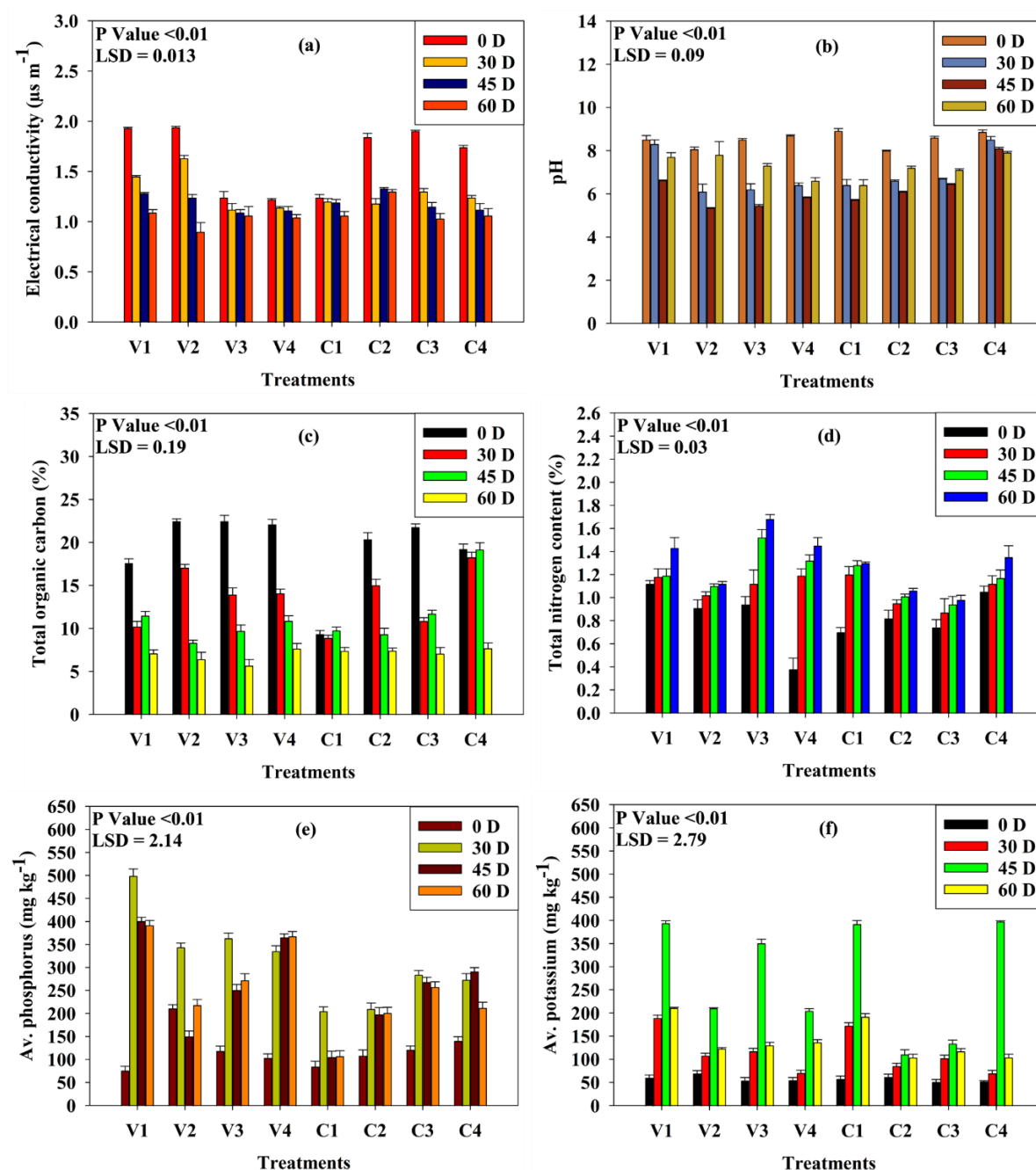


Figure 4.2: Dynamics of electrical conductivity (EC), pH, total organic carbon (TOC), total N (TN), and the availability of P and K in different lignocellulosic feedstocks. Values represent the mean±standard deviation (n = 3) for all the attributes. a. EC; b. pH; c. TOC; d. TN; e. Available phosphorus; and f. Available potassium

Correspondingly, the bioavailability of P and K after 60 days of incubation increased remarkably under vermicomposting compared with composting (Fig. 4.2e–f). At 60 days, the K-availability among the LCW (PS and FW)-based feedstocks was

significantly higher in V4 than in any of the others ($P_{\text{treatment}} < 0.01$; $\text{LSD} = 2.79$). Therefore, earthworms enhanced the population of K-solubilizing microorganisms in the vermibeds [20]. Correspondingly, the P availability was higher in V4 than in any other PS/FW-based feedstock under composting or vermicomposting ($\text{LSD} = 2.14$). Earthworms significantly contributed to P-enrichment by modifying the pH and elevating the growth of P-solubilizing microorganisms [11]

4.3.4. Dynamics of microbial biomass carbon, microbial respiration, and bacterial and fungal counts

The temporal variations in MBC, MR, and populations of bacteria and fungi during composting and vermicomposting are presented in Fig 4.3. MBC increased significantly in all composting and vermicomposting reactors until 45 days. However, the final MBC was highest in V4 [PS+FW(1:1)v], followed by V3 [(PS+FW+CD(3:3:2)v] and V2 [(PS+FW+CD(2:2:1)v] ($P_{\text{treatment}} < 0.01$; $\text{LSD} = 22.39$). Augmentation of microbial populations and their metabolic activity is a crucial feature of earthworm-mediated systems [12]. Thus, it can be postulated that the earthworms confronted the decay resistance of lignocellulosic macromolecules in the PS- and FW-dominated feedstocks by enhancing microbial loading in this study. MR increased substantially over time in the PS- and FW-based feedstocks that were vermicomposted and at 60 d highest MR was recorded in V3 followed by V4, V1, and V2 ($P_{\text{treatment}} < 0.01$; $\text{LSD} = 0.84$; Fig. 4.3b).

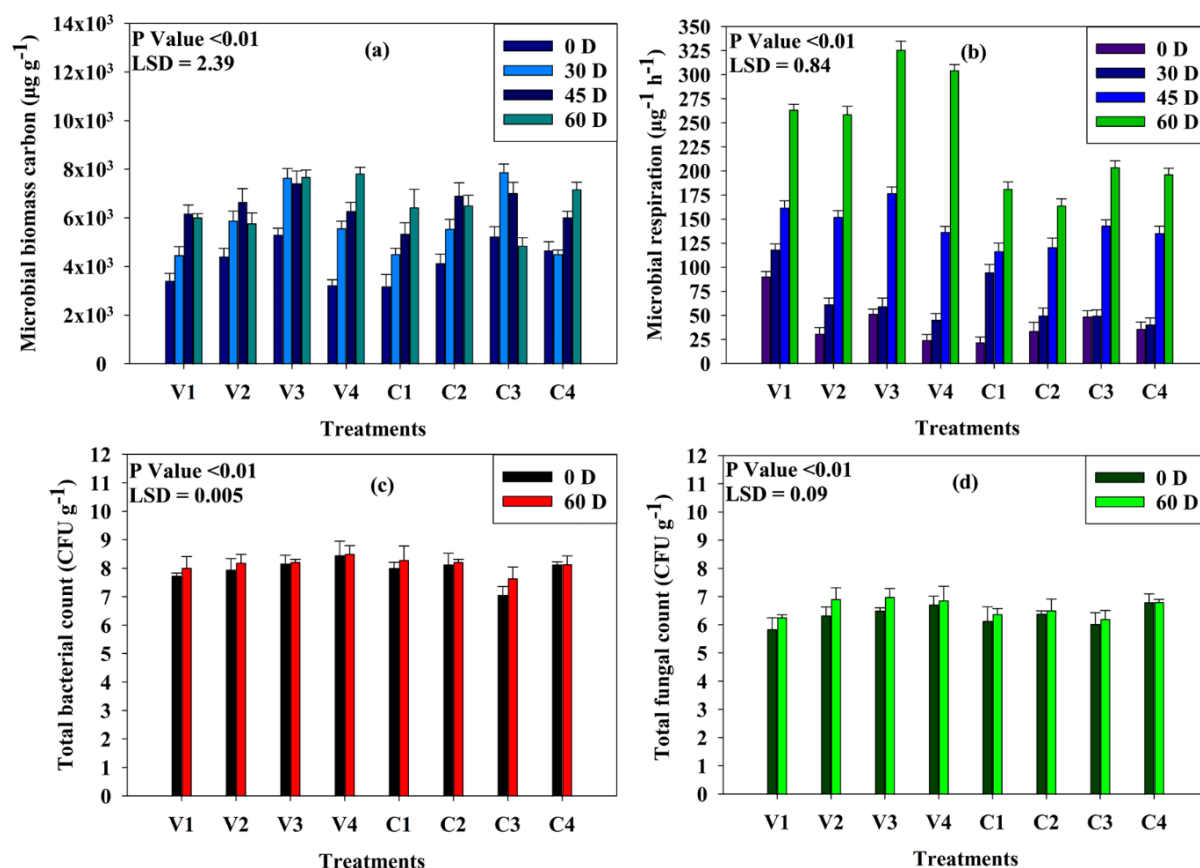


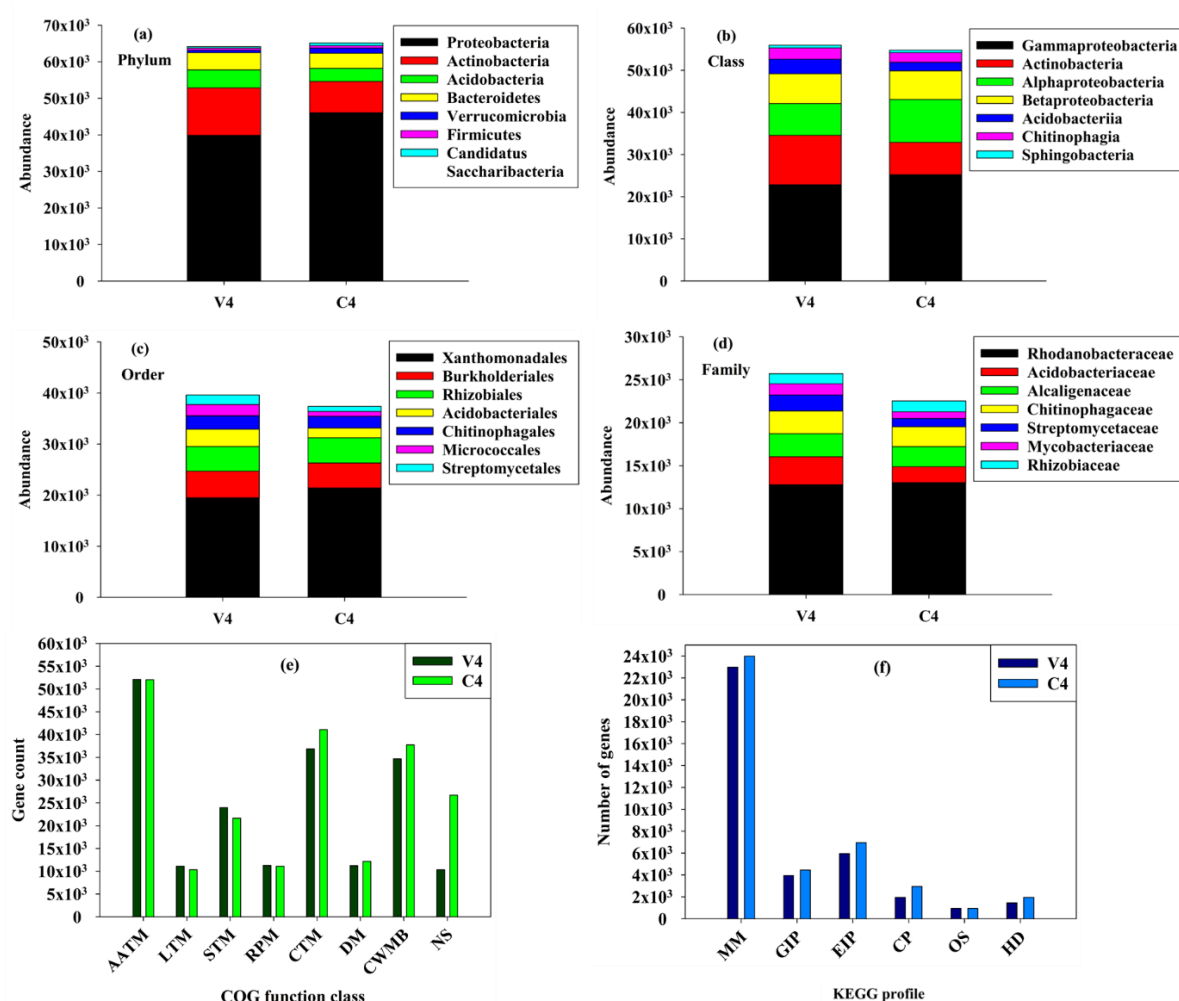
Figure 4.3: Variations in microbial attributes of feedstocks during composting and vermicomposting. Values represent the mean \pm standard deviation ($n = 3$) for all the attributes. a. Microbial biomass carbon (MBC); b. Compost respiration; c. Total bacterial count; and d. Total fungal count.

The treatment (i.e., feedstock) \times time interaction was also significant ($P < 0.01$) for MR and MBC, signifying a feedstock-induced effect on microbial growth. Interestingly, MR was significantly higher in the V4 and V3 vermibeds than in the other treatment beds at 60 days. The MR increase in the vermibeds is explained by the growth of beneficial zygomonas microflora [39]. Therefore, earthworm-induced aeration and microbial augmentation intensely activated zygomonas microflora in the PS+FW(1:1)v feedstock, promoting biomass mineralization. Correspondingly, the bacterial count increased significantly over time ($P_{\text{time}} < 0.01$) and at the end, it became the highest in PS+FW(1:1)v (i.e., V4) (Fig. 4.3c; $P_{\text{treatment}} < 0.01$; LSD=0.005). Similarly, the fungal population in various feedstocks at 60 d was in the order: V3=V4>V2>C4>C2>V1=C1>C3 (Fig. 4.3d; $P_{\text{treatment}} < 0.01$; LSD=0.03). These results clarify that microbial enrichment via earthworm interventions was the primary cause of the significantly greater nutrient mobilization in recalcitrant lignocellulosic waste found

in the vermicomposting system over the aerobic composting system [11]. Therefore, we applied advanced metagenomic analyses to reveal the actual value of earthworms in waste valorization.

4.3.5. Taxonomic and functional diversity in compost and vermicompost: Next generation sequencing–based analyses

The results of the NGS-based taxonomic analyses are presented in Fig. 4.4 and 4.5. Signatures of about 343.54 and 285.76 million DNA (i.e., reads) were primarily detected in LCW_v and LCW_c, respectively, and the total number of N50 scaffolds was greater in the vermicompost (LCW_v) samples than in the compost (LCW_c) samples. This finding implies that the number of overlapping DNA segments (i.e., contigs) was greater in the vermibeds (in the presence of earthworms) than in the composting beds [40]. The Illumina-based NGS results show that the abundance of the microbial communities differed noticeably between compost and vermicompost. Although *Proteobacteria* were the most dominant phyla (~60% of all genes) in both compost (LCW_c) and vermicompost (LCW_v) samples, members of *Actinobacteria*, *Acidobacteria*, and *Bacteroidetes* were much higher in the LCW_v samples than the LCW_c samples (Fig. 4.4a). The predominance of *Actinobacteria* and *Acidobacteria* was also greater under vermicomposting (LCW_v) than composting (LCW_c) at the phylum level (Fig. 4.4a). In contrast, *Proteobacteria*, *Verrucomicrobia*, and *Armatimonadetes* phyla were more prevalent in LCW_c feedstock than LCW_v feedstock. In other words, the microbial community profiles in the feedstocks were significantly altered by the presence of earthworms. However, *Beta-proteobacteria* was dominant in the vermicompost (LCW_v); while the *Alpha-proteobacteria* were more prevalent in the compost (LCW_c) than the vermicompost (LCW_v) at the class level (Fig. 4.4b).



AATM: Amino acid transport metabolism; LTM: Lipid transport metabolism; STM: Signal transduction mechanism; RPM: RNA processing and modification; CTM: Carbohydrate transport and metabolism; DM: Defense mechanisms; CWMB: Cell wall/membrane/envelope biogenesis; NS: Nuclear structure; MM: Metabolism; GIP: Genetic information processing; EIP: Environmental information processing; CP: Cellular processes; OS: Organismal systems; HD: Human diseases.

Figure 4.4: Taxonomic and functional diversity of microbial communities in compost and vermicompost at various taxa: a. Phyla; b. Class; c. Order; d. Family; e. Distribution of functional genes based on COG-derived databases; and f. Distribution of functional genes based on KEGG-derived databases.

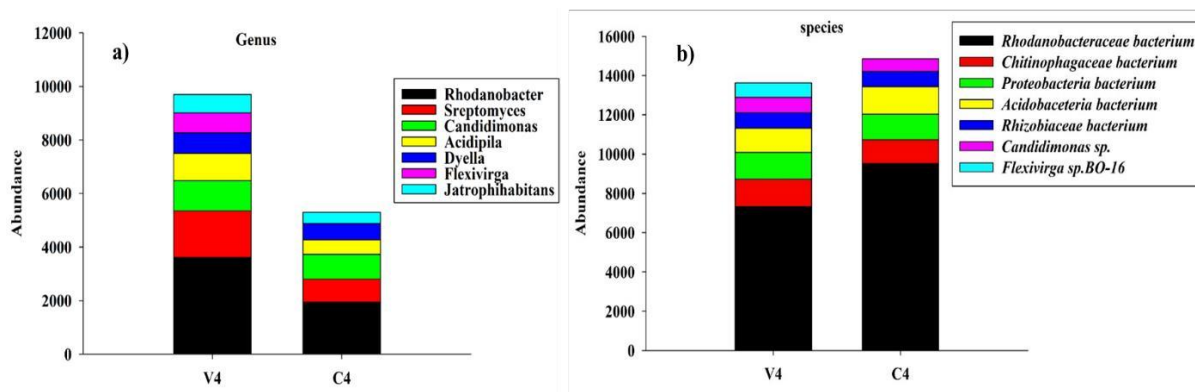


Figure 4.5: Variation in abundance of microbial genes in V4 and C4 feedstocks during the incubation period at various taxa: a. Genus; b. Species

Overall, the diversity of microbial orders (*Xanthomonadales*, *Burkholderiales*, *Rhizobiales*, and *Acidobacteriales*) was greater in the vermicompost (LCW_v) than the compost (LCW_c) (Fig. 4.4c). On the other hand, at the family level, *Acidobacteriaceae*, *Rhizobiaceae*, *Alcaligenaceae*, *Chitinophagaceae*, *Streptomycetaceae*, and *Mycobacteriaceae* were significantly more dominant in LCW_v than LCW_c (Fig. 4.4d). The variations in microbial taxa between the composted and vermicomposted feedstocks were also more spectacular at the genus and species levels (fig. 4.5 a and b). Interestingly, several members of the *Rhizobiaceae* and *Chitinophagaceae* families exhibit plant-growth-promoting traits [41]. The variations in microbial taxa between the composted and vermicomposted feedstocks were more spectacular at the genus and species levels (fig. 4.5 a and b). Fascinatingly, genes of a few species, such as *Beijerinckia* spp. and *Propionibacteriaceae* were exclusively found in LCW_v , among which *Beijerinckia* spp. are well-known, free-living, N-fixing bacteria [42].

The distribution of functional genes in the composted (LCW_c) and vermicomposted (LCW_v) samples was characterized based on the Clusters of Orthologous Groups of Proteins (COG) (Fig. 4.4e) and Kyoto Encyclopedia of Genes and Genomes (KEGG) (Fig. 4.4f–i) databases. The COG database focuses on the phylogenetic classification of functional proteins encoded in the genomes of bacteria, eukaryotes, and archaea, making it an effective tool for identifying microbial groups that possess multi-domain proteins [43]. KEGG, on the other hand, is a widely used molecular function database capable of performing functional annotation for all types of microorganisms [44]. Like the taxonomic profiles, significant variations in functional genes were observed between the groups. Six KEGG and 23 COG approaches were detected in LCW_v and LCW_c . The

genes linked to amino acid transport and metabolism, signal transduction mechanism, and RNA processing were greater in LCW_v than in LCW_c. Moreover, genes associated with nuclear structure development were found only in LCW_v. In contrast, genes related to carbohydrate transport, defense mechanisms, and biogenesis of cell walls and membranes were higher in LCW_c than LCW_v. It was reported that the community compositions and metabolic functions of microbiomes differ significantly depending on the presence or absence of earthworms in composting beds [12,18]. Therefore, the changes are induced by earthworm gut microbiota. Dominguez et al. (2021) [45] found that earthworms' guts eliminate more than 90% of their microbiome via their profuse excretion system. In this study, the growth of specific microbial communities containing biomass-degrading functional proteins and their associated genes were found to be augmented in the vermicomposting system. Therefore, we postulate that earthworm proliferation and activity in the vermireactors promoted the growth of specific microbial groups that ultimately accelerated LCW-mineralization processes during vermicomposting.

4.3.6. Waste conversion efficacy and economic evaluations

The industrial feasibility and environmental sustainability of vermicomposting could only be appreciated by evaluating the studied systems' waste-to-wealth conversion efficiency and economic potential. Our previous studies demonstrated that toxic metals and odorous volatiles in waste materials are significantly neutralized through vermicomposting [21,46]. Accordingly, the possibilities of emissions of obnoxious gases and migration of toxic metals from the end product (i.e., vermicompost) were negligible. Therefore, we have computed waste conversion (Table 4.6). WCE for vermicomposting was significantly higher than composting. These results indicate that vermicomposting is a better waste conversion route than aerobic composting. Still, the overall efficiency of these waste conversion treatments can only be assessed through the economic evaluation [47]. The enumerated benefit-cost ratio (BCR) for different processes is presented in Table 4.6

Table 4.6: Waste-to-wealth conversion efficiency (WCE) and benefit-cost ratio (BCR) for bio-composting systems and vermicomposting systems.

Treatments	WCE %	Benefit cost ratio (BCR)
Compost	61.8±1.33	0.651±0.003
Vermicompost	70.93±3.91	1.898±0.008
P-Value	<0.01	<0.01

The vermicompost production rate was assumed for 100 kg initial feedstock. However, the productivity and the cost of production were computed based on the real- time data acquired during the experiments (Table 4.4). Interestingly, the BCR was highest for the vermicomposting systems then the aerobic mediated composting system (1.898±0.008; $P < 0.05$).

4.4. Conclusion

A distinctive benefit of *Eisenia*-mediated vermicomposting of recalcitrant biomass over simple aerobic composting has been manifested in this research. The NGS-derived information revealed that earthworms improved bacterial communities (*Beijerinckiaceae* and *Propionibacteriaceae*) and greatly enhanced soil quality. Moreover, the predominance of functional genes (RNA processing, amino acid/lipid transport, and nuclear structure development) was higher in vermicompost (LCW_v) than in compost (LCW_c). These results allowed us to target a suitable feedstock that harbors potent plant- growth-promoting microbial communities. Conventionally, microbial metagenomic analyses are used to interpret microbial diversity and community shifts in response to change in the immediate environment. Such knowledge is rarely applied to generate microbial resources. Hence this study is the first proof-of-concept for using metagenomic approaches to locate ideal habitats from which to isolate economically viable microorganisms in line with researchers' interests.

Bibliography

- [1] Das, S., Lee, S. H., Kumar, P., Kim, K. H., Lee, S. S., Bhattacharya, S. S. "Solid Waste Management: Scope and the Challenge of Sustainability." *Journal of Cleaner Production*, 228: 658-678, 2019.
- [2] Poskart, A., Skrzyniarz, M., Sajdak, M., Zajemska, M., Skibiński, A. "Management of Lignocellulosic Waste towards Energy Recovery by Pyrolysis in the Framework of Circular Economy Strategy." *Energies*, 14: 1-17, 2021.
- [3] Sarsaiya, S., Jain, A., Kumar Awasthi, S., Duan, Y., Kumar Awasthi, M., Shi, J. "Microbial Dynamics for Lignocellulosic Waste Bioconversion and Its Importance with Modern Circular Economy, Challenges, and Future Perspectives." *Bioresource Technology*, 291: 121905, 2019.
- [4] United Nations Environment Programme. *Food Waste Index Report 2024*. Nairobi: United Nations Environment Programme, 2024.
- [5] Wu, D., Wei, Z., Qu, F., Mohamed, T. A., Zhu, L., Zhao, Y., Jia, L., Zhao, R., Liu, L., Li, P. "Effect of Fenton Pretreatment Combined with Bacteria Inoculation on Humic Substances Formation during Lignocellulosic Biomass Composting Derived from Rice Straw." *Bioresource Technology*, 303: 122849, 2020.
- [6] Pagliaccia, P., Gallipoli, A., Gianico, A., Gironi, F., Montecchio, D., Pastore, C., di Bitonto, L., Braguglia, C. M. "Variability of Food Waste Chemical Composition: Impact of Thermal Pre-Treatment on Lignocellulosic Matrix and Anaerobic Biodegradability." *Journal of Environmental Management*, 236: 100-107, 2019.
- [7] Ju, X., Engelhard, M., Zhang, X. "An Advanced Understanding of the Specific Effects of Xylan and Surface Lignin Contents on Enzymatic Hydrolysis of Lignocellulosic Biomass." *Bioresource Technology*, 132: 137-145, 2013.
- [8] Maitan-Alfenas, G. P., Visser, E. M., Guimarães, V. M. "Enzymatic Hydrolysis of Lignocellulosic Biomass: Converting Food Waste in Valuable Products." *Current Opinion in Food Science*, 1: 44-49, 2015.
- [9] Gil, A. "Current Insights into Lignocellulose Related Waste Valorization." *Chemical Engineering Journal Advances*, 8: 100186, 2021.

- [10] Bhattacharya, S. S., Iftikar, W., Sahariah, B., Chattopadhyay, G. N. "Vermicomposting Converts Fly Ash to Enrich Soil Fertility and Sustain Crop Growth in Red and Lateritic Soils." *Resource Conservation and Recycling*, 65: 100- 106, 2012.
- [11] Hussain, N., Singh, A., Saha, S., Venkata Satish Kumar, M., Bhattacharyya, P., Bhattacharya, S. S. "Excellent N-Fixing and P-Solubilizing Traits in Earthworm Gut-Isolated Bacteria: A Vermicompost Based Assessment with Vegetable Market Waste and Rice Straw Feed Mixtures." *Bioresource Technology*, 222:165-174, 2016.
- [12] Domínguez, J., Aira, M., Kolbe, A. R., Gómez-Brandón, M., omiérrez-Losada, M. "Changes in the Composition and Function of Bacterial Communities during Vermicomposting May Explain Beneficial Properties of Vermicompost." *Scientific Reports*, 9: (1), 1-11, 2019.
- [13] Paul, S., Goswami, L., Pegu, R., Kumar Chatterjee, S., Sundar Bhattacharya, S. "Epigenetic Regulations Enhance Adaptability and Valorization Efficiency in *Eisenia Fetida* and *Eudrilus Eugeniae* during Vermicomposting of Textile Sludge: Insights on Repair Mechanisms of Metal-Induced Genetic Damage and Oxidative Stress." *Bioresource Technology*, 345: 126493, 2022.
- [14] Devi, C., Khwairakpam, M. "Management of Lignocellulosic Green Waste Saccharum Spontaneum through Vermicomposting with Cow Dung." *Waste Management*, 113: 88-95, 2020.
- [15] Benitez, E., Sainz, H., Melgar, R., Nogales, R. "Vermicomposting of a Lignocellulosic Waste from Olive Oil Industry: A Pilot Scale Study." *Waste Management & Research*, 20: (2),134-142, 2002.
- [16] Sharma, K., Garg, V. K. "Recycling of Lignocellulosic Waste as Vermicompost Using Earthworm *Eisenia Fetida*." *Environmental Science and Pollution Research*, 26: 14024-14035, 2019.
- [17] Domínguez, J., Aira, M., Crandall, K. A., Pérez-Losada, M. "Earthworms Drastically Change Fungal and Bacterial Communities during Vermicomposting of Sewage Sludge." *Scientific Reports*, 11:1-10, 2021.

- [18] Pérez-Losada, M., Narayanan, D. B., Kolbe, A. R., Ramos-Tapia, I., Castro-Nallar, E., Crandall, K. A., Domínguez, J. "Comparative Analysis of Metagenomics and Metataxonomics for the Characterization of Vermicompost Microbiomes." *Frontiers in Microbiology*, 13: 854423, 2022.
- [19] Hussain, N., Das, S., Goswami, L., Das, P., Sahariah, B., Bhattacharya, S. S. "Intensification of Vermitechnology for Kitchen Vegetable Waste and Paddy Straw Employing Earthworm Consortium: Assessment of Maturity Time, Microbial Community Structure, and Economic Benefit." *Journal of Cleaner Production*, 182: 414-426, 2018.
- [20] Karmegam, N., Vijayan, P., Prakash, M., John Paul, J. A. "Vermicomposting of Paper Industry Sludge with Cow Dung and Green Manure Plants Using *Eisenia Fetida*: A Viable Option for Cleaner and Enriched Vermicompost Production." *Journal of Cleaner Production*, 228: 718-728, 2019.
- [21] Sahariah, B., Goswami, L., Kim, K. H., Bhattacharyya, P., Bhattacharya, S. S. "Metal Remediation and Biodegradation Potential of Earthworm Species on Municipal Solid Waste: A Parallel Analysis between *Metaphire Posthuma* and *Eisenia Fetida*." *Bioresource Technology*, 180: 230-236, 2015.
- [22] Page, A. L., Miller, R. H., Keeney, D. R. *Methods of Soil Analysis, in: Chemical and Microbiological Properties*. Madison, Wisconsin, USA, 1982.
- [23] Bélanger, N., Pare, D., Hendershot, W. H. "Determining Nutrient Availability in Forest Soils." *Soil Sampling and Methods of Analysis: Second Edition*, 317-329, 2007.
- [24] Sasmal, S., Goud, V. V., Mohanty, K. Characterization of biomasses available in the region of North-East India for production of biofuels. *Biomass and Bioenergy*, 45:212-220, 2012.
- [25] Nelson, D. W., Sommer, L. E. Total Carbon, Organic Carbon and Organic Matter. *Methods of Soil Analysis, Part 2. Chemical and Microbiological Properties*, 2nd edition. 1982.
- [26] Epstein, E. *The Science of Composting*. CRC Press LLC, Florida, 504 p., 1997.

- [27] Jenkinson, D. S. "The Determination of Microbial Biomass Carbon and Nitrogen in Soil." In: Wilson, J. R., Ed., *Advances in Nitrogen Cycling in Agricultural Ecosystems*, CAB International, Wallingford, 368-386, 1988.
- [28] Parmer, C., Schmidt, A. "Organic Matter." In: *Methods of Soil Analysis, Part-I*. C. A. Black (ed.). American Society of Agronomy Madison, USA, 1395-1397, 1964.
- [29] Chattopadhyay, G. N. *Chemical Analysis of Fish Pond Soil and Water*. Daya Books, 1998.
- [30] Kutchko, B. G., Kim, A. G. "Fly Ash Characterization by SEM–EDS." *Fuel*, 85: (17-18), 2537-2544, 2006.
- [31] Head, S. R., Komori, H. K., LaMere, S. A., Whisenant, T., Van Nieuwerburgh, F., Salomon, D. R., Ordoukhanian, P. Library construction for next-generation sequencing: overviews and challenges. *Biotechniques*, 56: (2), 61-77. 2014.
- [32] Ghosh, S., Das, A. P. "Metagenomic Insights into the Microbial Diversity in Manganese-Contaminated Mine Tailings and Their Role in Biogeochemical Cycling of Manganese." *Scientific Reports*, 8: 8257, 2018.
- [33] Hussain, N., Das, S., Goswami, L., Das, P., Sahariah, B., Bhattacharya, S. S. Intensification of vermitechnology for kitchen vegetable waste and paddy straw employing earthworm consortium: assessment of maturity time, microbial community structure, and economic benefit. *Journal of Cleaner Production*, 182: 414-426. 2018.
- [34] U.S. Environmental Protection Agency (USEPA). *Soil Sampling Quality Assurance User's Guide*. Environmental Monitoring System Laboratory, Las Vegas, 1989.
- [35] Lalander, C. H., Fidjeland, J., Diener, S., Eriksson, S., Vinnerås, B. "High Waste-to-Biomass Conversion and Efficient Salmonella spp. Reduction Using Black Soldier Fly for Waste Recycling." *Agroecology and Sustainable Food Systems*, 39: (3), 261– 271, 2015.
- [36] Dillon, J. L., Hardaker, J. B. *Farm Management Research for Small Farmer Development*. Food and Agriculture Organization (FAO) of the United Nations, 6, 1993.

- [37] Mondal, A., Goswami, L., Hussain, N., Barman, S., Kalita, E., Bhattacharyya, P., Bhattacharya, S. S. "Detoxification and Eco-Friendly Recycling of Brick Kiln Coal Ash Using *Eisenia fetida*: A Clean Approach through Vermitechnology." *Chemosphere*, 244: 125470, 2020.
- [38] Edwards, C. A., Lofty, J. R. *Biology of Earthworms*. Chapman & Hall, London, 283 pp., 1972.
- [39] Dilly, O. "Microbial Energetics in Soils." *Microorganisms in Soils: Roles in Genesis and Functions. Soil Biology*, 3: 123–138, 2005.
- [40] Fullwood, M. J., Wei, C. L., Liu, E. T., Ruan, Y. "Next-Generation DNA Sequencing of Paired-End Tags (PET) for Transcriptome and Genome Analyses." *Genome Research*, 19: 521–532, 2009.
- [41] Madhaiyan, M., Poonguzhali, S., Senthilkumar, M., Pragatheswari, D., Lee, J. S Lee, K. C. "*Arachidicoccus rhizosphaerae* gen. Nov., sp. nov., a Plant-Growth-Promoting Bacterium in the Family Chitinophagaceae Isolated from Rhizosphere Soil." *International Journal of Systematic and Evolutionary Microbiology*, 65: 578–586, 2015.
- [42] Morawe, M., Hoeke, H., Wissenbach, D. K., Lentendu, G., Wubet, T., Kröber, E., Kolb, S. "Acidotolerant Bacteria and Fungi as a Sink of Methanol-Derived Carbon in a Deciduous Forest Soil." *Frontiers in Microbiology*, 8: 1–18, 2017.
- [43] Tatusov, R. L., Galperin, M. Y., Natale, D. A., Koonin, E. V. "The COG Database: A Tool for Genome-Scale Analysis of Protein Functions and Evolution." *Nucleic Acids Research*, 28: 33–36, 2000.
- [44] Zhang, C., Chen, Z., Zhang, M., Jia, S. "KEGG_Extractor: An Effective Extraction Tool for KEGG Orthologs." *Genes*, 14: 386, 2023.
- [45] Domínguez, J., Aira, M., Crandall, K. A., Pérez-Losada, M. "Earthworms Drastically Change Fungal and Bacterial Communities During Vermicomposting of Sewage Sludge." *Scientific Reports*, 11:(1), 15556, 2021.
- [46] Paul, S., Choudhury, M., Deb, U., Pegu, R., Das, S., Bhattacharya, S. S. "Assessing the Ecological Impacts of Ageing on Hazard Potential of Solid Waste Landfills: A

Green Approach through Vermitechnology." *Journal of Cleaner Production*, 236: 117643, 2019.

- [47] Pata, S. U. K., Kartal, M. T., Adebayo, T. S. "Enhancing Environmental Quality in the United States by Linking Biomass Energy Consumption and Load Capacity Factor." *Geoscience Frontiers*, 14: (3), 2023.